FIBER PROPERTIES OF SELECTED COTTON LINES OBTAINED BY MUTAGENESIS

E. Hequet and N. Abidi
International Textile Center
Texas Tech University
Lubbock, TX
D. Auld
Department of Plant and Soil Sciences
Texas Tech University
Lubbock, TX

Abstract

Mutagenesis was accomplished by exposing imbibed seed to a 3% v/v concentration of Ethyl Methanesulfonate (EMS). Four mutant lines, the parent variety and a control were evaluated for their physical properties. The mutant lines were replicated three times in the field, while the parent line and the control were replicated 6 times. Macrostructural and microstructural investigations were done, in order to explain the differences in the physical properties observed among the mutant lines.

Introduction

The purpose of this work was to investigate the macrostructure and the microstructure of cotton fibers from selected lines obtained by mutagenesis (Auld et al, 1998 ; Auld et al, 2000). The relationships among the data obtained and the physical properties of the cotton fibers were studied. Scanning Electron Microscopy (SEM) and image analysis of the cross-sections of the fibers were performed to evaluate the cotton fibers' macrostructures. This enabled evaluation of the morphology of the fibers, the cellulose deposition within the fibers along with fiber maturity, and fiber diameter. The microstructure was investigated by X-Ray diffraction to evaluate the crystallinity and the crystallite orientation. Information gained from the macrostructural and microstructural studies should enable us to establish a relationship between fiber structure and physical properties such as bundle tenacity, elongation, maturity, etc.

Materials and Methods

Four mutant lines, along with the parent variety (HS200) and the control (HS26) were evaluated using the Zellweger Uster Advanced Fiber Information System (AFIS) and the Zellweger Uster High Volume Instrument 900A (HVI). The mutant lines were replicated three times in the field and the parent line and the control six times. For each fiber sample 5 replications of 3,000 fibers were performed on the AFIS. On the HVI, 4 color and micronaire readings along with 10 length and strength readings were performed.

The morphological investigations were carried out using SEM. The cotton fibers were deposited on the sample-holder, coated with a layer of gold by means of thermal evaporation in a vacuum coating unit, and examined in the SEM using an accelerating voltage of 20 KV. Ten pictures from each sample were taken at a magnification of 3,000.

Then image analysis was performed using 3 replications of approximately 500 fibers. The method used here was developed at the Southern Regional Research Center in New Orleans, Louisiana, USA (Boylston et al., 1995). It uses a methacrylate polymer to hold the cotton fibers in order to cut them with a rotary microtome into 1-micron slices, then mounting on glass slides for observation. Approximately 500 fibers are captured in each sample. The prepared glass slides were viewed with a computerized video microscope, which captures the magnified images and stores them in computer files. These images then remain available for use in measuring area and perimeter of the fibers. The software package developed by Bugao Xu, University of Texas at Austin, was used to take the computerized measurements of the fiber cross-sections.

The micro structural study was achieved using X- Ray Diffraction (XRD). The XRD patterns were collected on bundles of parallel fibers using a Rigaku X-ray diffractometer. Crystallinity, crystallite orientation and texture were determined. Six fiber samples were selected for XRD. They consisted of cottons samples from the following varieties or lines: HS200, HS26, TTU271, 271-215C, TTU202, 202-1170B. One ramie (*Boehmeria nivea*) fiber sample was included as a control, ramie being known to be highly crystalline and oriented.

Results and Discussion

Physical Properties: AFIS and HVI

Tables 1 and 2 summarize the results obtained.

When measured with the AFIS, the mutant lines are not statistically different from the parent line for the number of neps and seed coat fragments. As expected, both the mean length (Lw) and the Upper Quartile Length (UQL) are better for the mutants, TTU202 being the longest. There are no significant differences between the lines tested for the Short Fiber Content by weight (SFCw). It was expected that fibers with the longest UQL would exhibit the lowest SFCw. The fact that it was not confirmed may indicate a problem with the fiber length distribution, this, in turn, could have a negative impact on the yarn quality, especially the number of imperfections and the yarn hairiness. The maturity ratios (MR) are not significantly different, but the standard fineness measurements indicate slightly finer fiber for the line TTU271.

When measured with the HVI, the 4 mutant lines exhibit longer Upper Half Mean Length (UHML) than the parent line, confirming the AFIS results. Nevertheless, the ranking is slightly different. The Uniformity Index (UI) is slightly better for TTU202. For the strength readings, TTU271 has the highest strength, followed by TTU202. TTU271 exhibits the lowest elongation. The micronaire of TTU271 is the lowest, followed by TTU202. This indicates that the highest HVI bundle strength exhibited by those two lines may not be related to intrinsically stronger individual fibers but rather to a larger number of fibers in the bundle.

Fiber Macrostructure Analyses

Scanning Electron Microscopy (SEM). Figure 1 shows the SEM pictures at the same magnification (3,000 X) of selected fibers. These figures show the typical dimensional structure variation in cotton fibers. The surface wrinkles in sample TTU271 seem to be oriented nearly in the axis of the fiber, while the samples TTU202, 202-170B, 271-2155C, and HS26 are not (arrows indicate the direction of surface wrinkles). If we assume that the wrinkles of the primary wall are revealing, at least partially, the underlying structure, TTU271 should have higher fiber strength.

Image Analysis of Fiber Cross-Sections. The image analysis of the fiber cross-section allows determination of the fiber perimeter, area of the cross section and maturity (Theta). The table 3 shows respectively the results obtained on the 4 mutant lines, along with the varieties HS26 and HS200. TTU202 has the largest perimeter along with one of the lowest maturity demonstrating that the high HVI bundle strength obtained on this line is probably not due to intrinsic higher fiber strength. The line 271-2155C (reselection from TTU271) exhibits one of the lowest perimeter along with one of the highest maturity and a good HVI length along with a good strength. This line is probably the more balanced among the four lines. This means that some residual variability still exists in the line TTU271. A reselection of this line to try to obtain a line with the length and the strength

Reprinted from the *Proceedings of the Beltwide Cotton Conference*
Volume 2:1247-1250 (2001)
National Cotton Council, Memphis TN

of TTU271 along with the fiber perimeter and the maturity of 271-2155C is probably possible.

Fiber Microstructure Analysis

A Rigaku X-ray diffractometer was used to collect the data for these measurements. The bundles of fibers were mounted on a rigid holder and the data were collected under specific conditions to eliminate preferred orientation effects. Figure 2 gives the XRD patterns of selected fibers. The percentage of crystallinity (Crystallinity Index) was calculated from the XRD patterns by using the following equation (Wakida et al, 2000):

$$\% \text{ Crystallinity} = \frac{I_c}{I_a + I_c} x100$$

Where I_c represents the integrated diffraction intensity of crystalline regions, and I_a represents the integrated diffraction intensity of the amorphous region.

The percentage of crystallinity of selected samples is given in table 4. Ramie sample has the highest percentage of crystallinity as expected, along with sample TTU202 and TTU271, while 202-1170B have the lowest percentage of crystallinity.

The on-axis frames from Ramie and sample TTU202 (figure 3) show the (002) set of planes (C-axis) oriented equatorial to the fiber axis. The sharpness of the reflections observed in the XRD-diagram of ramie indicates a high crystallinity and orientation. However, the XRD-diagram of TTU202 appears more diffuse which indicates less crystallinity and orientation.

The measurement of texture for polycrystalline materials can be performed by X-ray diffraction techniques. "For the accurate determination of crystalline texture, the technique of pole figure diffractometry is required. The much simpler method of powder diffractometry can produce ambiguous and misleading results" (Dittmar, 1991). This is the reason why we chose to study fiber bundles rather than fiber powder. The texture strength is quantified by integrating the (002) equatorial reflections along the Debye ring, and the full-width-at-half-maximum (FWHM) is reported in the table 4. FWHM of any reflection indicates the texture strength since all sets of lattice planes are related. In general, the larger is the FWHM, the weaker is the texture. In this case, 271-2155C has the weaker texture while TTU271 has the strongest.

The orientation angles were calculated from the Herman orientation function relative to the fiber axis (Lewin et al, 1998).

Table 5 summarizes the orientation angles of the crystallites relative to the fiber axis. Smaller is the value the higher is the orientation relative to the fiber axis. Therefore, the fiber is expected to be stronger. This is the case of the sample TTU271.

It should be pointed out, however, that some source of error could be introduced in sample preparation and mounting. In fact, the texture measurements were performed on small bundles of fibers rather than on single fibers. This could introduce a source of error, since it is very difficult to align the fibers exactly in the same direction, so the bundle will have some angular spread around the fiber axis.

Conclusion

All the indications gathered (from HVI, AFIS, SEM, Cross-section image analysis, and XRD) are going in the same direction; the line TTU271 has the best-balanced fiber properties.

Acknowledgment

Funding for this project was provided by the Texas Cotton Biotechnology Initiative - TxCot.

References

Auld, D.L., R.G. Cantrell, E. Bechere, E.F. Hequet. 2000. Inheritance of fiber length in two mutants of cotton. *Proceedings of the Beltwide Cotton Conference*, Vol. 1, 518-520.

Auld, D.L., M.D. Ethridge, J.K. Dever, J.D. Dotray. 1998. Chemical mutagenesis as a tool in cotton improvement. Proceedings of the Beltwide Cotton Conference, Vol. 1, 550-552.

Boylston, E. K., J.P. Evans and D.P. Thibodeaux. 1995. A quick embedding method for light microscopy and image analysis of cotton fibers. Biotechnic and Histochemistry 70 (1):24-27.

Dittmar, M, B. The role of X-ray diffraction in the control of sputtering target crystal texture. In. Microelectronics manufacturing technology, V14(6), June 1991.

Reimschuessel, H. K. 1998. in "*Handbook of Fiber Chemistry*" Edited by M. Lewin and E. M. Pearce. Page 96

Wakida, T, Y. Kitamura, M, Lee, S. Bae, M. Chen, H. Yoshika, and Y. Yanai. 2000. Effect of hot water processing on dyeing and chemical properties of cottons treated with liquid ammonia and sodium hydroxide. *Textile Res. J.* 70(9), 769-774.

Table 1. Mutant lines: HVI data.

Cotton	UHML Inch	UI %	Strength g/tex	Elongation %	Micronaire
HS26	1.140 c	83.5 ab	30.1 bc	7.7 a	3.92 ab
HS200	1.142 c	83.7 ab	29.7 c	7.6 a	3.98 ab
TTU271	1.227 a	83.1 b	32.3 a	7.0 b	3.63 b
271-2155C	1.210 ab	83.6 ab	31.0 abc	7.5 a	4.00 ab
TTU202	1.217 a	84.2 a	31.6 ab	7.6 a	3.77 ab
202-1170B	1.180 b	83.2 b	30.0 bc	7.4 a	4.13 a

Means in a column not followed by the same letter are significantly different.
Method of least significant differences ($P \leq 0.05$)

Table 2. Mutant lines: AFIS data.

Cotton	Nep Count	SCN Count	Lw Inch	SFCw %	UQL Inch	MR	Fine-ness mtex	Std. Fineness mtex
HS26	187a	22a	0.980c	8.2a	1.192c	0.870a	159ab	183a
HS200	200a	27a	0.988c	8.0a	1.198c	0.867a	159ab	184a
TTU271	224a	21a	1.037ab	8.4a	1.290ab	0.857a	154b	179b
271-2155C	181a	27a	1.037ab	7.5a	1.273ab	0.883a	160ab	181ab
TTU202	183a	25a	1.063a	7.6a	1.307a	0.873a	159ab	182ab
202-1170B	168a	28a	1.023b	8.1a	1.260b	0.887a	164a	185a

Means in a column not followed by the same letter are significantly different.
Method of least significant differences ($P \leq 0.05$)

Table 3. Mutant lines: Image Analysis of fiber cross-sections data.

Cotton	Area micron^2	Perimeter micron	Theta
HS26	96.5b	50.0ab	0.508ab
HS200	99.7ab	49.8b	0.525a
TTU271	89.4c	49.3b	0.484b
271-2155C	98.5ab	49.6b	0.521ab
TTU202	98.3ab	51.4a	0.490ab
202-1170B	104.3a	50.5ab	0.531a

Means in a column not followed by the same letter are significantly different.
Method of least significant differences ($P \leq 0.05$)

Table 4. X-Ray Diffraction data.

Sample	% Crystallinity	FWHM (002)
HS26	51	63
HS200	54	64
TTU271	55	59
271-2155C	49	69
TTU202	55	66
202-1170B	46	60
Ramie	57	14.6

Table 5. X-Ray Diffraction data.

Sample	Orientation angle
HS26	38.94
HS200	39.33
TTU271	38.31
271-2155C	39.72
TTU202	38.78
202-1170B	39.21
Ramie	33.10

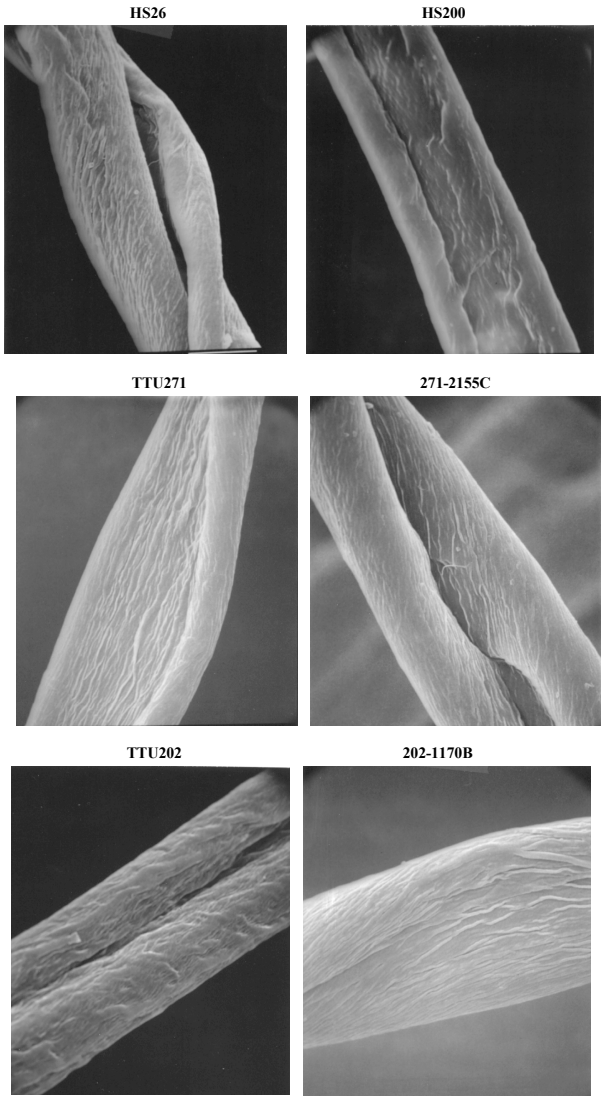

Figure 1: Scanning Electron Microscopy of selected cotton fibers

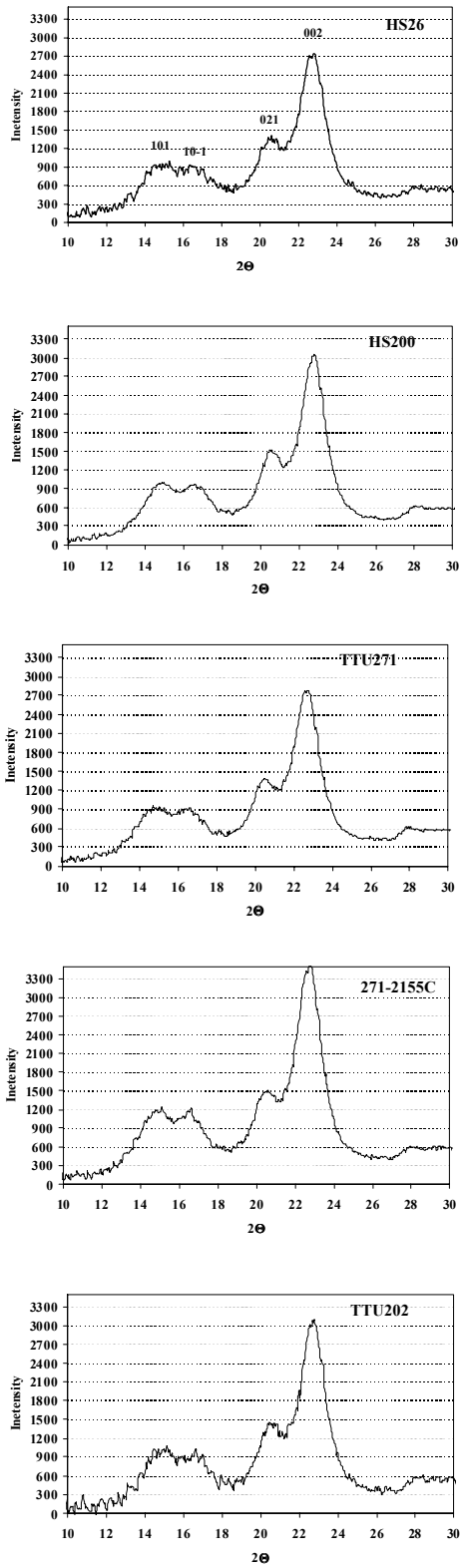

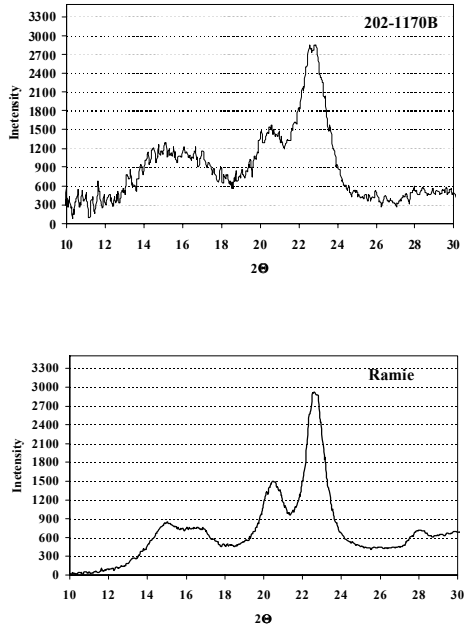

Figure 2: XRD patterns of selected cotton fibers

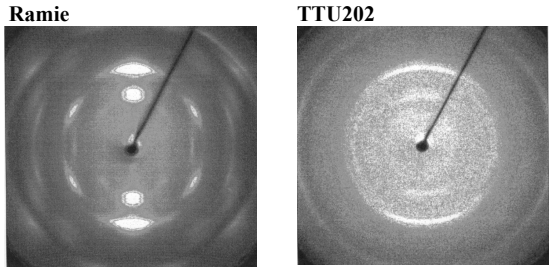

Figure 3: On axis image of Ramie and TTU202 cotton fibers